Hindawi Publishing Corporation
Journal of Sensors
Volume 2015, Article ID 151859, 6 pages
http://dx.doi.org/10.1155/2015/151859

Hindawi

Research Article

A Wearable Contactless Sensor Suitable for Continuous Simultaneous Monitoring of Respiration and Cardiac Activity

Gaetano D. Gargiulo,[1] Upul Gunawardana,[2] Aiden O'Loughlin,[3] Mohammad Sadozai,[2] Elham Shabani Varaki,[1] and Paul P. Breen[1]

[1]*The MARCS Institute, University of Western Sydney, Penrith, NSW 2750, Australia*
[2]*School of Computing Engineering and Mathematics, University of Western Sydney, Penrith, NSW 2750, Australia*
[3]*School of Medicine, University of Western Sydney, Campbelltown, NSW 2560, Australia*

Correspondence should be addressed to Gaetano D. Gargiulo; g.gargiulo@uws.edu.au

Received 29 July 2015; Revised 26 August 2015; Accepted 27 August 2015

Academic Editor: Hyeonseok Yoon

A reliable system that can simultaneously and accurately monitor respiration and cardiac output would have great utility in healthcare applications. In this paper we present a novel approach to creating such a system. This noninvasive, low power, low cost, contactless sensor is suitable for continuous monitoring of respiration (tidal volume) and cardiac stroke volume. Furthermore, it is capable of delivering this data in true volume (i.e., mL). The current embodiment, specifically designed for sleep monitoring applications, requires only 100 mW when powered by a 4.8 V battery pack and is based on the use of a single electroresistive band embedded in a T-shirt. Here, we describe the implementation of the device, explaining the rational and design choices for the electronic circuit and the physical garment together with the preliminary tests performed using one volunteer subject. Comparison of the device with a commercially available spirometer demonstrates that tidal volume can be monitored over extended periods with a precision of ±10%. We further demonstrate the utility of the device to measure cardiac output and respiration effort.

1. Introduction

Monitoring of respiration patterns and the identification of respiratory abnormalities are an important clinical task [1, 2], particularly during sleep which may account for roughly 1/3 of one's lifetime. For this reason, a number of sensors suitable for respiration pattern monitoring during sleep have been reported. Some of these sensors require skin contact (e.g., systems that utilize electrodes like impedance plethysmography), while others are based on calibrated displacement sensors or inductive sensors that are embedded in tightly fitted jackets/garments (e.g., inductive plethysmography and strain-gauge plethysmography) [3–11].

Inductive and strain-gauge plethysmography systems allow easy detection of breathing pattern disruption and are commonly employed as part of more complex "sleep disorders" monitoring systems [11, 12]. Respiratory effort is an important measurement particularly during sleep as the differences in phase between chest and abdomen movements during respiration (or attempted respiration) are linked to obstructive apnoea and other sleep disorders [1, 11, 13, 14].

Along with respiration, the correct measurement of cardiac stroke is a crucial parameter. This value when multiplied by the heart rate allows the calculation of the cardiac output and when monitored in conjunction with tidal volume completes the hemodynamic general assessment summary [15, 16]. Impedance plethysmography is the only current noninvasive technology that is capable of monitoring respiration and simultaneously approximating cardiac function, in particular cardiac stroke volume [17]. However, impedance plethysmography is computationally intensive and requires a large number of electrodes connected in a precise arrangement and an electrical signal to be injected into the body [9]. For this reason, there is a growing demand

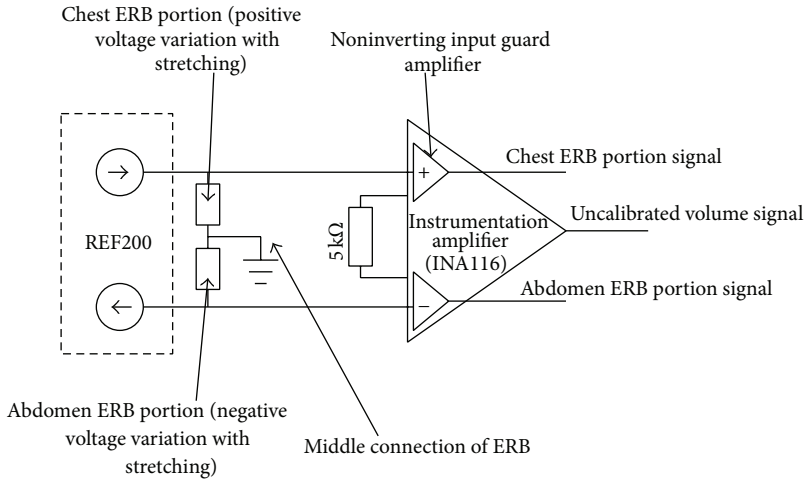

Figure 1: ERB front-end mark II principle diagram.

for precise noninvasive continuous measurement of cardiac output, particularly with simultaneous recording of tidal volume and respiratory effort.

Our previous implementation of this sensor [18] already allows monitoring of respiration and measures cardiac stroke volume directly in millilitres without the need to infer these measurements from a mathematical model (e.g., as a conical frustum) [12, 17, 19].

With the aim of achieving simultaneous measurement of cardiac stroke volume, tidal volume, and respiratory effort in a contactless wearable solution suitable for use during sleep, we investigated the use of commercially available electroresistive bands (ERBs) [18]. These bands are normally used for electromagnetic shield gaskets and also as cheap displacement/force sensor in robotic projects. The electroresistive bands that we employed are made of highly elastic conductive silicone (carbon loaded) tubes. They have a thickness of 2 mm and are sold at an approximate length of 1 m. At rest they exhibit a total resistance in the range of 6 to 7 kΩ, and when stretched their resistance varies in the range of 140 to 160 Ω per cm. In this paper we examine the feasibility of using a single ERB to monitor tidal volume, cardiac stroke volume, and respiratory effort during sleep. Once again, for descriptive purposes we refer to this device and its subsequent recording as a pneumocardiogram (PNCG) [18].

2. Methods

In a previously described embodiment of this sensor [18], we employed four ERBs arranged in pairs, two over the chest and two over the abdomen, placed in the same areas where the stiff ribbon is sewn (see Figure 2). The sensor and the electronics designed for this previous embodiment allowed us to demonstrate that the sensor is suitable for long-term PNCG recording and also during intense physical activity. However, this implementation had two drawbacks. First, multiple ERBs required the use of a multichannel bespoke ERB front end. Second, in our previous design the ERBs were arranged around the entire torso. The extension of the sensing area at the back of the rib cage impaired the use of the sensor when a portion of the ERB was compressed or pinched which occurred when the user lies down. The current implementation aims to address simultaneously both of these issues.

2.1. ERB Front-End Mark II. Similar to our previous design [18], our single ERB is polarized using a small DC current. The required DC current is achieved using a single microchip: the REF200 by Texas Instruments [20]. This configuration of a single ERB and REF200 allows us to avoid fine regulation of the polarization current, contrary to our previous designs where, due to the presence of multiple bands individually polarized, to avoid microshock hazard [4] we required adjusting the current level to values different from 100 μA (of note, the standard value for microshock threshold is 100 μA).

To still allow monitoring of chest and abdomen area, in this implementation the ERB is divided into two equal length portions (chest and abdomen; see wearable garment section). The middle point is connected to the circuit ground (see Figure 1) and both portions of the ERB are polarized independently by the single REF200 which contains two independent current generators.

Summation of ERB voltages (uncalibrated volume signal; see Figure 1) is achieved directly by an analogue circuit using a true differential amplifier (INA116 also by Texas Instruments [21]). To sum both voltages, we forced the ERB connected to the differential amplifier inverting input to generate a negative voltage variation with respect to ground when stretching. Negative voltage compliance for the current generators is achieved using an isolated DC-DC converter module (DHC10512D by TI) which generates a dual unregulated rail power supply of up to ±14 V from a single power supply of 4.8 V (5 V power supply nominal specification). For this application we powered our prototypes using the 5 V output from the National Instruments NI6009 which was also used to acquire the data at a sampling rate of 1000 Hz. Although the signal output of the INA116 does not require amplification, in order to accommodate the low dynamic range of the ADC used during our tests (14 bits in a ±5 V),

Table 1: Bill of material comparison.

Component type	ERB front-end mark I [18]	ERB front-end mark II
Instrumentation amplifier	4 (INA118)	1 (INA116)
Current bias generator	2 (REF200)	1 (REF200)
Operational amplifier	4 (OPA129)	None
Power supply	1 (DHC10512D)	1 (DHC10512D)
Passive resistors	12 (several different values)	1 (5 kΩ)
Capacitors	1 (2.2 μF); 2 (10 μF); 16 (100 nF)	1 (2.2 μF); 2 (10 μF); 2 (100 nF)
ERB	4 (1 m)	1 (1 m)

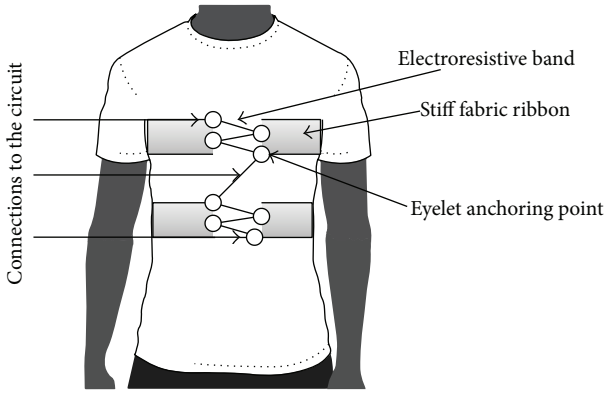

Figure 2: Schematic representation of the garment (see text).

a gain of 11 V/V is achieved by directly connecting a 5 kΩ resistor between pins 1 and 8 of the INA116.

Independent instrumentation and measurement of chest and abdomen movements during respiration (respiratory effort) are achieved by the guard buffers integrated into the INA116 [21]. Normally guard buffers are used to polarize the shield of the coaxial cable connected to the sensors with a replica of the sensed signal. This technique, known as an active guard setup (for more details see [22–25]), is commonly used to minimize noise capture in the cable and connections to sensors. However, because ERBs work at very low frequency (almost at DC level) and due to the intrinsic high resistance that they exhibit, they do not offer a preferable pathway for noise coupling. For this reason, in this application the ERB is connected to the circuitry with a two-conductor shielded cable (commonly used for earphones), with the shield connected to the middle point of the ERB and to the signal ground (see Figure 1). This arrangement leaves the guard buffer outputs free, allowing us to use them to directly read the voltage signals of each portion of the ERB. The result of all this is that using only one microchip we are able to extract three useful analogue signals. Direct comparison between the bills of material for the current and previously used front ends is reported in Table 1.

2.2. Wearable Garment Mark II. The wearable garment implemented for this trial is depicted in Figure 2. Once again, we have used a loose fit T-shirt as a base for the garment. In the chest area (between the armpits) and in the abdomen area (floating ribs) a 5 cm wide stiff fabric ribbon is sewn leaving a gap of 7 cm. Some nonconductive eyelets were embedded in the ribbon near the edge of the gap (see Figure 2). The ERB is then treaded through the eyelets in a zigzag pattern. The ERB is secured with knots at the right topmost eyelet and at the left bottommost eyelet of each ribbon. Connection of the ERB to the polarization circuit and the noninverting input of the instrumentation amplifier is achieved at the topmost eyelet while the inverting input of the INA116 and polarizing circuit is connected to the ERB at the lowest eyelet. The ground connection is secured with a crimp terminal at the middle point of the ERB. The ERB is loosely stitched to the fabric to avoid shorting the section and unwanted stretching of that connection trunk. In this implementation a simple two-core coaxial cable (normally used for earphones) is used to connect the garment to the measurement circuit. As in our previous implementation of the garment, calibration of the voltage variation associated with the sum of the chest and abdomen ERB portions to chest true volume is performed against three measurements taken with a commercial spirometer. A polynomial interpolation (second-order) was obtained by curve fitting the three measurements from the summed ERB and the spirometer recording (MATLAB basic fitting tool).

2.3. The Evaluation Setup. In this experiment, the prototype T-shirt was worn for several hours while data was recorded in two separate trials in parallel with recordings from the spirometer and a single ECG lead (MLI or modified lead I [16]) similar to what was implemented in [26, 27]. The first trial was used for calibration and initial assessment, while the second was used to estimate how well the calibration held after several hours. In both trials the volunteer was lying on a standard household bed and was occasionally asked to breathe through the spirometer used for calibration.

During the first trial the first three breathing cycles (intentionally different) have been used for calibration. After two hours, another cycle of recordings was made. The volunteer returned to bed after two further hours to take further measurements.

3. Results

Precision versus the spirometer after calibration was computed from a number of measurements taken during the two hours following the calibration (subject lying on a standard

Table 2: Test and calibration measurements values.

Spirometer reading [mL]	Sensor reading [mL]	Error (%)
Test measurements after calibration		
1670	1620	3
2890	2775	4
3300	3040	8
1660	1670	−1
Test measurements trial 2 (see text)		
2000	2132	−7
1610	1770	−10
1660	1810	−9
1750	1711	2
2210	2425	−10
2880	3020	−5

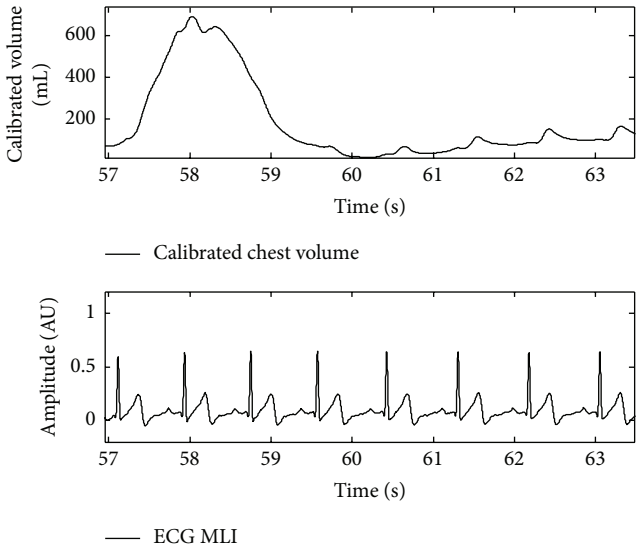

Figure 3: Data excerpt representing one normal breathing cycle followed by slow inspiration to demonstrate cardiac stroke volume dependence on respiration.

household bed) and in the second trial when the subject was asked to lie on the bed again after two hours. The subject did not remove the T-shirt in the intertrials period that was spent performing standard daily activities. Results from these measurements are reported in Table 2 and show that the error versus the spirometer is contained in the range of ±10%.

An excerpt of calibrated data recorded during Trial 1 is depicted in Figure 3. For this particular recording, the subject was asked to take a single shallow breath and perform a slow inspiration. The purpose of this recording is to show dependence of the cardiac stroke volume on respiration as would be expected. As it is possible to observe in Figure 4 top panel, a small volume variation is observable that corresponds with each cardiac beat (Figure 1 bottom panel). Although such dependence is expected, as is a delay between the electrical activity of the heart (ECG) and the changes in volume resulting from the pumping action, we assume that there is a further delay added by the response time of the

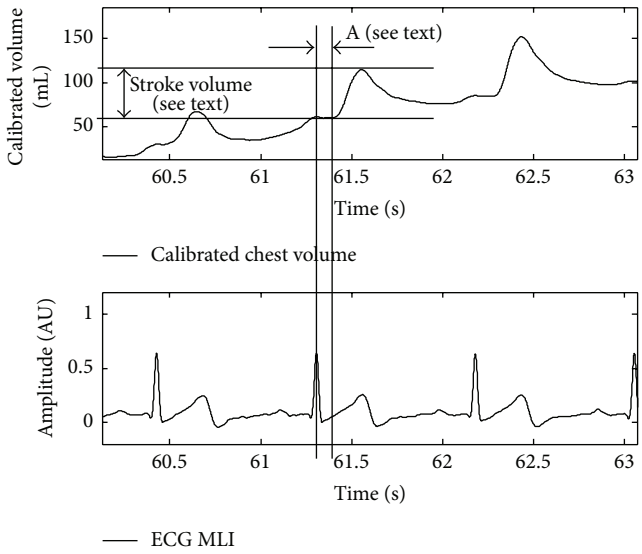

Figure 4: Magnified section of data represented in Figure 3.

ERBs. For this reason, the time interval that in Figure 4 is marked with "A" measured as time interval between the peak of the QRS and the local minima of the volume signal may be larger than normal physiological values of ~30 ms [4, 28]; see Section 4. Similarly, the cardiac stroke volume is measured as peak-to-peak value between the first local minima and the first local maxima after the heart beat (see Figure 4) may be influenced by the delay and damping impressed by the ERB as well as by the amplitude modulation impressed by the respiration. As evaluation of precision of our sensor for cardiac stroke volume involves invasive procedure, we are currently in the process of obtaining ethical clearance to test our prototype in a hospital that routinely performs such procedure.

The capability of our new sensor implementation to assess respiratory effort is demonstrated during the performance of some simulated sleep apnoea events. In this experiment, to generate a simulated apnoea event, the subject attempted respiration following forced expiration. As it is possible to observe by comparing Figures 5 and 6, during normal respiration (Figure 5) the chest and abdomen are synchronized and in phase (please note that by circuit design the abdomen ERB section voltage variation is negative) while during apnoea (Figure 6) there is loss of synchronization and chest expansions are spasmodic as they are driven by chest superficial muscles rather than respiration muscles. Therefore, despite using a single ERB in this implementation this sensor is still capable of monitoring respiratory effort.

Lastly, we highlight that by simple comparison of the two bills of material (Table 1) it is possible to infer that the front-end mark II is cheaper as expensive components such as instrumentation amplifiers are reduced from four to one and expensive operational amplifiers (OPA129) previously used are no longer required. Furthermore, as fine regulation of the polarizing current for each of the bands is no longer required, accurate and time consuming calibration is no longer needed.

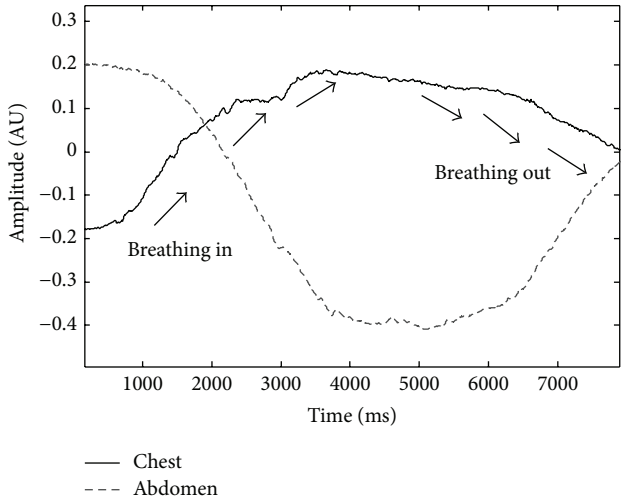

Figure 5: Respiratory effort (normal breathing cycle).

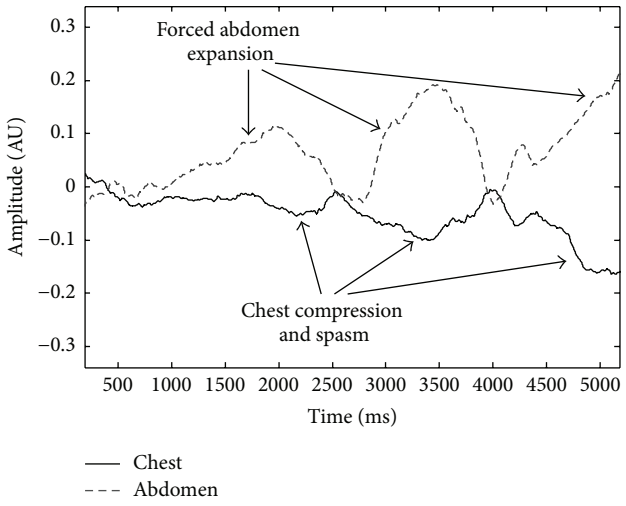

Figure 6: Respiratory effort (simulated apnoea; see text).

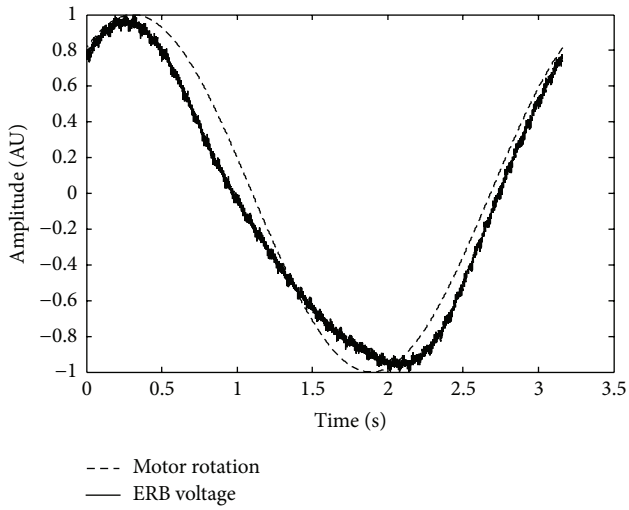

Figure 7: Direct comparison of motor rotation pattern and voltage variation of ERB raw data (stretching percentage ~10%).

4. Discussion

ERBs employed in our prototype are commercially available from Adafruit Industries (New York, USA) and specifically designed to perform as displacement sensors in robotic applications. As mentioned in Section 3, the delay between the ECG signal (QRS) and volume gradient measured by our system (see Figures 3 and 4) is larger than the standard physiological delay. This delay is due to the ERB material. As expected, the changes in resistance in the ERBs are also due to a thermal effect and to the nonlinear concentration of the conductive compound (carbon powder).

Although the impact that the delay has upon the measurements of stroke volume will be evaluated only during the scheduled clinical measurements (2016), we assessed the delay and shape of the ERB voltage variation when polarized by currents of levels as used in this application simulating long-term monitoring (>10 hours of continues stretching) at stretching frequencies similar to respiration (in a range between 0.2 and 0.5 [Hz]). We also found that the performances of the ERBs degrade if they are overstretched. In our application the garment is designed to contain the stretching below 10%. With a stretching of 10% we found that the delay affects mostly the relaxation of the band and is contained in the 10% of the stretching speed. An example of our characterization measurements is depicted in Figure 7.

In order to test the ERBs we built a test system formed by a high-torque slow revolution (geared) DC motor connected directly to an adjustable rigid arm (to stretch one end of the ERB) and via a belt to a high precision rotary encoder (2000 pulses per turn). The sinusoidal waveform (dashed bold line) is obtained by the rotary encoder pulses that have been acquired simultaneously with the voltage variation of the ERB by a National Instruments DAQpad6363 sampling at 25 kHz. In order to acquire data precisely at each turn, the DAQpad acquisition is triggered by the single revolution phase of the rotary encoder. Residual high-frequency noise visible on the ERB voltage in Figure 7 is due to the absence of a proper low-pass filter at the input of the DAQpad. Of note, our low-pass filter is currently calibrated for a sample rate of 1000 Hz that is currently employed for the human trial recordings.

5. Conclusion

The presented device represents a significant step toward the development of a solution for noninvasive simultaneous measurement of respiration and cardiac function. This technology has several significant advantages: it can be easily embedded in existing wearable long-term monitoring solutions (e.g., Holter monitors) and, being contactless, it can be worn over bandages or electrodes and remain effective. Furthermore, although only one ERB is employed for this design, the device can still monitor the respiratory effort broadening its use to sleep monitoring and disordered breathing monitoring. Future work will focus on development and characterization of the electroresistive bands,

validation of cardiac output measurement (comparison with invasive measurements), and larger scale studies of long-term reliability.

Conflict of Interests

The authors declare that there is no conflict of interests regarding the publication of this paper.

References

[1] K. E. Barrett, S. M. Barman, S. Boitano, and H. L. Brooks, *Ganong's Review of Medical Physiology*, McGraw-Hill Medical, 23rd edition, 2009.

[2] D. Prutchi and M. Norris, *Design and Development of Medical Electronic Instrumentation: A Practical Perspective of the Design, Construction, and Test of Medical Devices*, 2004.

[3] D. W. Cartwright, G. A. Gregory, and M. M. Willis, "A respiratory function jacket for measuring tidal volume and changes in FRC," *Journal of Applied Physiology Respiratory Environmental and Exercise Physiology*, vol. 55, no. 1, pp. 263–266, 1983.

[4] J. G. Webster, Ed., *Medical Instrumentation Application and Design*, John Wiley, Hoboken, NJ, USA, 2009.

[5] T. Uhlig, T. Kondo, and P. D. Sly, "Measurements of PEEP-induced changes in lung volume: evaluation of a laser monitor," *Chest*, vol. 112, no. 1, pp. 107–112, 1997.

[6] J. E. Yount, "Easily calibrated circumferential respiratory effort transducer with low mechanical load and medium impedance," in *Proceedings of the Annual International Conference of the IEEE Engineering in Medicine and Biology Society*, November 1989.

[7] R. Paradiso and D. D. Rossi, "Advances in textile technologies for unobtrusive monitoring of vital parameters and movements," in *Proceedings of the 28th IEEE EMBS Annual International Conference*, New York, NY, USA, 2006.

[8] R. J. Thomas, "Arousals in sleep-disordered breathing: patterns and implications," *Sleep*, vol. 26, no. 8, pp. 1042–1047, 2003.

[9] M. Akay, *Wiley Encyclopedia of Biomedical Engineering*, John Wiley & Sons, Hoboken, NJ, USA, 2006.

[10] K. Brown, C. Aun, E. Jackson, A. Mackersie, D. Hatch, and J. Stocks, "Validation of respiratory inductive plethysmography using the Qualitative Diagnostic Calibration method in anaesthetized infants," *European Respiratory Journal*, vol. 12, no. 4, pp. 935–943, 1998.

[11] Z. Zhang, J. Zheng, H. Wu, W. Wang, B. Wang, and H. Liu, "Development of a respiratory inductive plethysmography module supporting multiple sensors for wearable systems," *Sensors*, vol. 12, no. 10, pp. 13167–13184, 2012.

[12] K. Konno and J. Mead, "Measurement of the separate volume changes of rib cage and abdomen during breathing," *Journal of Applied Physiology*, vol. 22, no. 3, pp. 407–422, 1967.

[13] U. R. Acharya, E. C.-P. Chua, O. Faust, T.-C. Lim, and L. F. B. Lim, "Automated detection of sleep apnea from electrocardiogram signals using nonlinear parameters," *Physiological Measurement*, vol. 32, no. 3, pp. 287–303, 2011.

[14] R. U. Acharya, A. Kumar, P. S. Bhat et al., "Classification of cardiac abnormalities using heart rate signals," *Medical and Biological Engineering and Computing*, vol. 42, no. 3, pp. 288–293, 2004.

[15] G. R. Naik, Ed., *Recent Advances in Biomedical Engineering*, InTech, Rijeka, Croatia, 2009.

[16] R. O. Bonow, D. Mann, D. Zipes, and P. Libby, Eds., *Braunwald's Heart Disease: A Textbook of Cardiovascular Medicine*, Elsevier, 2012.

[17] D. P. Bernstein, "A new stroke volume equation for thoracic electrical bioimpedance: theory and rationale," *Critical Care Medicine*, vol. 14, no. 10, pp. 904–909, 1986.

[18] G. D. Gargiulo, A. O'Loughlin, and P. P. Breen, "Electro-resistive bands for non-invasive cardiac and respiration monitoring, a feasibility study," *Physiological Measurement*, vol. 36, no. 2, 2015.

[19] L. Borcea, "Electrical impedance tomography," *Inverse Problems*, vol. 18, no. 6, pp. R99–R136, 2002.

[20] Burr-Brown, "REF200 dual current source/sink," Technical Data, Burr-Brown, 1988.

[21] Burr-Brown, "INA116," Technical Data, Burr-Brown, 2008.

[22] P. Horowitz and W. Hill, *The Art of Electronics*, Cambridge University Press, Cambridge, UK, 2002.

[23] G. D. Gargiulo, J. Tapson, A. Van Schaik, A. McEwan, and A. Thiagalingam, "Unipolar ECG circuits: towards more precise cardiac event identification," in *Proceedings of the IEEE International Symposium on Circuits and Systems (ISCAS '13)*, pp. 662–665, Beijing, China, May 2013.

[24] G. D. Gargiulo, A. L. McEwan, P. Bifulco et al., "Towards true unipolar ECG recording without the Wilson central terminal (preliminary results)," *Physiological Measurement*, vol. 34, no. 9, pp. 991–1012, 2013.

[25] G. Gargiulo, R. Calvo, C. Jin et al., "Giga-ohm high-impedance FET input amplifiers for dry electrode biosensor circuits and systems," in *Integrated Microsystems: Electronics, Photonics, and Biotechnology*, K. Iniewski, Ed., CRC Press, 2011.

[26] G. Gargiulo, P. Bifulco, M. Cesarelli et al., "An ultra-high input impedance ECG amplifier for long-term monitoring of athletes," *Medical Devices: Evidence and Research*, vol. 3, no. 1, pp. 1–9, 2010.

[27] G. Gargiulo, P. Bifulco, R. A. Calvo, M. Cesarelli, C. Jin, and A. Van Schaik, "Mobile biomedical sensing with dry electrodes," in *Proceedings of the International Conference on Intelligent Sensors, Sensor Networks and Information Processing (ISSNIP '08)*, pp. 261–266, Sydney, Australia, December 2008.

[28] G. D. Gargiulo, R. W. Shephard, J. Tapson et al., "Pregnancy detection and monitoring in cattle via combined foetus electrocardiogram and phonocardiogram signal processing," *BMC Veterinary Research*, vol. 8, article 164, 2012.